Journal of Membrane Science and Research 1 (2015) 96-99

Journal of Membrane Science and Research

journal homepage: www.msrjournal.com

Short Communications

Hybrid Molten/Solid In_2O_3-Bi_2O_3 Oxygen Ion Transport Membranes

V.V. Belousov*, S.V. Fedorov, I.V. Kul`bakin

A.A. Baikov Institute of Metallurgy and Materials, Russian Academy of Sciences, 49 Leninskii Pr., 119991 Moscow, Russia

HIGHLIGHTS

- The hybrid molten/solid oxide membranes are developed.
- The overall oxygen permeation kinetics is controlled by chemical diffusion.
- The membranes show high oxygen permeability and selectivity.

GRAPHICAL ABSTRACT

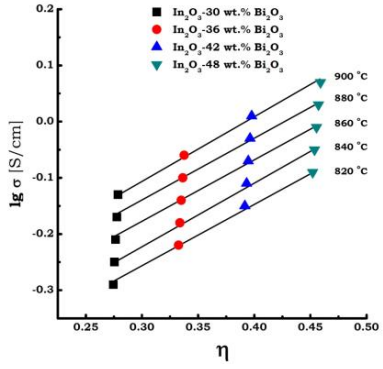

ARTICLE INFO

Article history:
Received 2014-08-11
Revised 2014-10-31
Accepted 2014-11-06
Available online 2014-11-06

Keywords:
Oxygen ion transport membranes
Solid/liquid oxide composites
Oxygen separation

ABSTRACT

The hybrid molten/solid In_2O_3 - 30-48 wt.% Bi_2O_3 oxide materials were studied with respect to their transport properties. The conductivities, oxygen ion transport numbers and oxygen permeation fluxes have been measured by using the four-probe DC, volumetric measurements of the faradaic efficiency and gas flow techniques, respectively. We show that the oxygen permeability of the hybrid molten/solid In_2O_3-Bi_2O_3 materials is comparable to that of the state-of-the-art oxygen ion transport membrane materials. In the ranges of temperatures between 820-900 °C and thicknesses 1.2-3.4 mm used in the present study, the overall oxygen permeation kinetics was controlled by chemical diffusion. The hybrid molten/solid materials show promise for use as ion transport membranes for oxygen separation from air.

1. Introduction

A central goal in the field of oxygen separation by ion transport membranes (ITM) [1] is to develop ductile membrane materials with high mixed ion-electronic conductivity. Recent studies have shown that some hybrid molten/solid oxide materials conduct both oxygen ions and electrons [2-6]. The hybrid molten/solid oxygen ion transport material design concept was proposed in References [7] and [8]. These materials consist of electron-conducting solid grains and ion-conducting liquid channels at the grain boundaries and are called the liquid-channel grain-boundary structures (LGBS). Under an oxygen electrochemical potential gradient, ambipolar conductivity of oxygen ions and electrons results in a high oxygen permeation rate through the LGBS materials [9,10]. Moreover, the intergranular liquid channels give the LGBS materials high mechanical plasticity [6] which would

* Corresponding author at: Tel./fax: + 7(499)1352-060
E-mail address: vbelousov@imet.ac.ru (V.V. Belousov)

make it easy to shape and alleviate problems due to brittleness [11]. The ductile hybrid molten/solid membrane materials are developing as an alternative to the brittle ceramic membrane materials.

The solid/liquid interfaces affect the transport properties of the hybrid molten/solid materials. In particular, the space charge regions with an enhanced ionic conductivity can form at the interfaces. Electrical and mass transfer along the interfaces is accompanied by changes in interfacial tension, which causes Marangoni flow and eases the transfer.

We have previously reported the oxygen permeation of $BiVO_4$-V_2O_5, ZrV_2O_7-V_2O_5 and ZnO-Bi_2O_3 LGBS materials [2-6]. Although these results are suggestive, the development of LGBS membrane materials with high oxygen permeability and selectivity is important. This paper focuses on the oxygen permeation of In_2O_3 - 30-48 wt.% Bi_2O_3 LGBS materials. We show that the oxygen permeability of the In_2O_3-Bi_2O_3 LGBS materials is comparable to that of the state-of-the-art membrane materials [12-15]. These hybrid molten/solid materials could be used as ITM for oxygen separation from air.

The samples were prepared for two stages: first – the ceramic sample preparation; second – the LGBS sample preparation. Source materials of our samples were In_2O_3 (99.9 %) and Bi_2O_3 (99.9 %) powders. In order to prepare the In_2O_3 - 30, 36, 42, and 48 wt.% Bi_2O_3 ceramic composites, the corresponding powder mixtures were grounded in a ball mill (Pulverisette-5, Germany) and were then compressed into disks (diameter of 25 mm and thickness of 1-5 mm) and parallelepipeds (5×5×40 mm) under 1.3 GPa pressure at room temperature, followed by sintering in air at temperatures below eutectic point (see Figure 1, ACerS-NIST PHASE EQUILIBRIA DIAGRAMS Version 3.1) for 15-24 h. The ZrV_2O_7 and $BiVO_4$ compound preparation details are described in Ref. [2].

In order to prepare the In_2O_3 - 30-48 wt.% Bi_2O_3 LGBS materials, the ceramic composites were then heated above eutectic point into a two-phase area of the In_2O_3-Bi_2O_3 phase diagram (marked area in Figure 1), where the solid In_2O_3 and liquid are in equilibrium. The microstructure of the samples was characterized by SEM (JSM-7401F, Japan) equipped with an EDX analyzer.

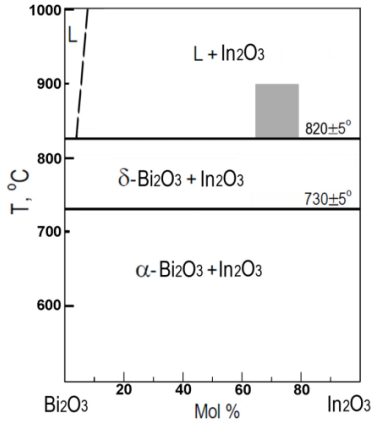

Fig. 1. Phase diagram of In_2O_3-Bi_2O_3.

Electrical conductivity of the samples (parallelepipeds) was measured as a function of temperature by the conventional four-probe DC technique in air. Since there is no reaction between platinum and oxide melt, one was used as material for electrodes. Distance between the probes was 20 mm.

Oxygen permeation fluxes and oxygen ion transference numbers of the samples (disks) were measured by gas flow and volumetric measurements of the faradaic efficiency techniques, respectively, in a specially designed cell, which is presented elsewhere [2]. The permeation area was 2.2 - 2.6 cm^2. The sample disk was fixed between two quartz tubes. The liquid phase on the sample surface ensured the gas-tight seal at high temperature. After sealing, air flowed at one side of the sample and helium at the opposite side. After reaching the steady state, the concentrations of oxygen and nitrogen in the sweeping gas flow were detected by gas chromatograph (Krystalluxe - 4000 M, Russia). The oxygen partial pressure at the surface of the oxygen-permeated sample side was changed by changing the sweeping gas flow rate from 5 to 20 ml/min. Leakage was controlled by measuring the trace oxygen and nitrogen contents in the isolation chamber. This mechanical leakage was concluded to be negligible, because the oxygen mechanical leakage rate was less than 1% of oxygen electrochemical permeation rate through the sample.

During the ceramic sample heating, a grain boundary wetting transition occurred at eutectic point [2-6,16-18]. The result was LGBS material consisting of In_2O_3 solid grains (dark constituent in Figure 2) and liquid channels at the grain boundaries (light constituent in Figure 2). The liquid phase includes both the molten Bi_2O_3 and In_2O_3 oxides. The intergranular liquid channels give the LGBS material high mechanical plasticity (see Figure 3). The ambipolar conductivity of oxygen ions by the molten Bi_2O_3 [19] and electrons by the solid In_2O_3 [20] results in an oxygen permeation through the LGBS material. Figures 4 and 5 show the liquid volume fraction dependences of the conductivity and ion transport number of the In_2O_3-Bi_2O_3 LGBS materials, respectively. Because liquid channels conduct predominantly oxygen ions [9], the oxygen ion transport number increases with the volume fraction of the liquid.

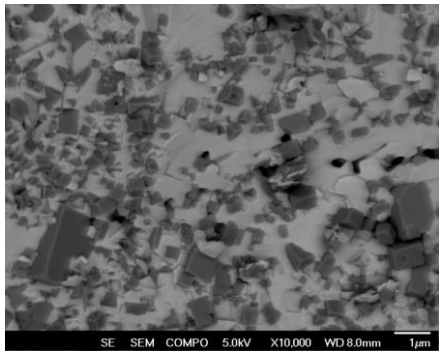

Fig. 2. Scanning electron micrograph of In_2O_3-48 wt.% Bi_2O_3 LGBS (after cooling from 840 °C).

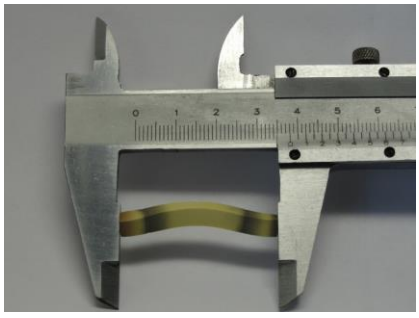

Fig. 3. Photography of In_2O_3-48 wt.% Bi_2O_3 LGBS after deformation at 840 °C.

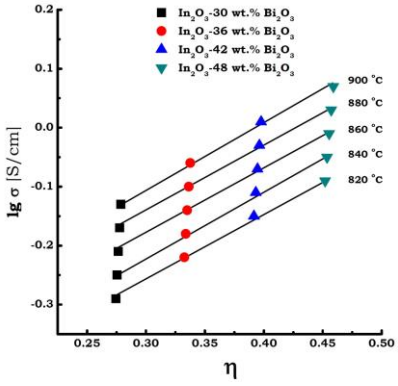

Fig. 4. Liquid volume fraction dependences of oxygen ion transport number of In_2O_3-Bi_2O_3 LGBS materials.

Figure 6 shows the oxygen permeation flux of the In_2O_3-Bi_2O_3 LGBS materials as a function of the volume fraction of liquid. The oxygen permeation flux increases with the volume fraction of liquid. As the volume fraction of liquid is in direct proportion to the Bi_2O_3 content (according to the In_2O_3-Bi_2O_3 phase diagram), the oxygen permeation flux increases with Bi_2O_3 content. The oxygen permeation flux through the In_2O_3 – 30-48 wt.% Bi_2O_3 LGBS membrane materials is varied from 6.7×10^{-8} to 8.6×10^{-8} mol/cm^2s (see Figure 6). However, at the same time, the nitrogen permeation flux (j_{N2}) through the membrane materials was practically equal to zero. This result indicates that the LGBS membrane materials have a very high oxygen selectivity $j_{O2}/j_{N2} \rightarrow \infty$.

The oxygen permeation through LGBS materials depends on three mechanisms: the first is the dissociation of oxygen molecules into oxygen anions at the LGBS material surface, known as surface exchange kinetics

[21]. The second is the migration of oxygen anions through the LGBS material, known as chemical diffusion [9], while the third is the recombination of oxygen anions back to oxygen molecules on the other side of the LGBS materials. Each mechanism has the potential to become the rate-limiting step. Wagner`s equation (1) is usually used to describe the oxygen permeation flux (j_{O2}) due to the chemical diffusion [6,9].

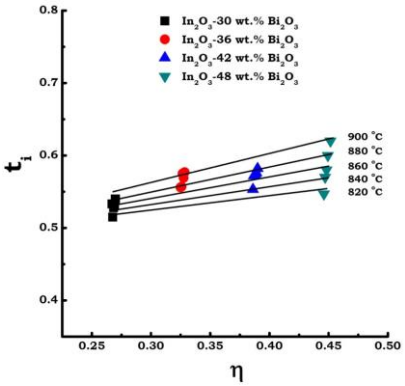

Fig. 5. Liquid volume fraction dependence of oxygen permeation flux of In_2O_3-Bi_2O_3 LGBS materials at 850°C ($\ln(P'_{O2}/P''_{O2})$) = 1.7, L = 0.2 cm).

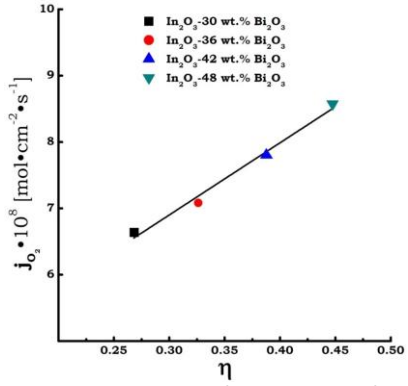

Fig. 6. Thickness dependence of oxygen permeation flux of In_2O_3 - 42 wt.% Bi_2O_3 LGBS material at 850°C ($\ln(P'_{O2}/P''_{O2})$) = 1.7).

$$j_{O_2} = \frac{RT}{16F^2L}\int_{\ln P''_{O_2}}^{\ln P'_{O_2}} \sigma_{amb}\, \mathrm{d}\ln P_{O_2} \quad (1)$$

$$\sigma_{amb} = \frac{\sigma_i\sigma_e}{\sigma_i+\sigma_e} = t_i t_e \sigma = t_i(1-t_i)\sigma \quad (2)$$

where σ_{amb}, σ, σ_i and σ_e are the ambipolar, overall, ionic and electronic conductivities, respectively, t_i and t_e are the oxygen ion and electron transference numbers, respectively, L is the LGBS material thickness, F is the Faraday constant, R is the universal gas constant, P'_{O2} and P''_{O2} are the oxygen partial pressure at the oxygen-rich and -lean sides of the LGBS material, respectively, and T is the temperature. Taking an average value of σ_{amb} simplifies Eq. (1) further so that j_{O2} is proportional to $\overline{\sigma_{amb}}$ and $\ln(P'_{O2}/P''_{O2})$.

$$j_{O_2} = \frac{RT}{16F^2L}\overline{\sigma_{amb}}\ln\frac{P'_{O_2}}{P''_{O_2}} \quad (3)$$

In order to determine whether chemical diffusion or the surface exchange reactions is the rate-limiting step in determining the overall oxygen permeation rate, the oxygen permeation fluxes were measured at different LGBS material thicknesses. Results of the thickness variation experiments are displayed in Figure 7. If oxygen permeation through the LGBS material is totally controlled by the chemical diffusion process as shown in Eq. (3), the oxygen permeation flux would have to be inversely proportional to the LGBS material thickness for a given oxygen partial pressure gradient. The linear relationship of the In_2O_3 - 42 wt.% Bi_2O_3 LGBS material indicates that the overall permeation kinetics is controlled by chemical diffusion.

In order to compare the membrane material performances, the oxygen permeability j^*_{O2} was calculated by formula (4)

$$j^*_{O_2} = j_{O_2}\frac{L}{\ln(P'_{O_2}/P''_{O_2})} \quad (4)$$

The values of the oxygen permeability of the In_2O_3 – 30-48 wt.% Bi_2O_3 LGBS materials at 850 °C are comparable to that of the state-of-the-art membrane materials (Table 1).

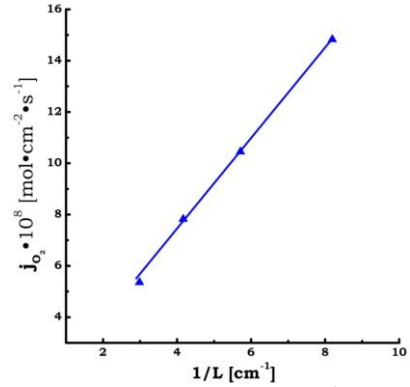

Fig. 7. Thickness (L) dependence of oxygen permeation flux j_{O2} of In_2O_3 - 42 wt.% Bi_2O_3 LGBS material at 850°C ($\ln(P'_{O2}/P''_{O2})$) = 1.7).

Table 1
The oxygen permeability j^*_{O2} of some membrane materials and In_2O_3 – 48 wt.% Bi_2O_3 LGBS.

Membrane material	T, K	j_{O_2}, mol cm^{-2} s^{-1}	L, mm	P_{O_2}, atm	P'_{O_2}, atm	$j^*_{O_2}$, mol cm^{-1} s^{-1}	References
$Pr_{0.6}Sr_{0.4}Co_{0.5}Fe_{0.5}O_{3-\delta}$	1173	$2.3\cdot10^{-7}$	0.6	0.21	0.001	$5.7\cdot10^{-9}$	[12]
$Ba_{0.5}Sr_{0.5}Co_{0.8}Fe_{0.2}O_{3-\delta}$	1173	$1.7\cdot10^{-6}$	1.3	0.21	0.001	$2.9\cdot10^{-8}$	[22]
$La_{0.6}Ca_{0.4}Co_{0.8}Fe_{0.2}O_{3-\delta}$	1173	$1.2\cdot10^{-7}$	1.0	0.20	0.0053	$3.3\cdot10^{-9}$	[23]
In_2O_3-48wt.%Bi_2O_3 LGBS	1123	$8.7\cdot10^{-8}$	2.0	0.21	0.038	$1.0\cdot10^{-8}$	

Acknowledgments

This work was supported by Russian Foundation of Basic Research.

Refernces

[1] A.C. Bose, G.J. Stiegel, P.A. Armstrong, B.J. Halper, E.P. Foster, Progress in ion transport membranes for gas separation application. In: A.C. Bose (Ed.), Inorganic membranes for energy and environmental application, Springer, New York, 2009.
[2] S.V. Fedorov, V.V. Belousov, A.V. Vorobiev, Transport properties of $BiVO_4$ – V_2O_5 liquid-channel grain-boundary structures, J. Electrochem. Soc. 155 (2008) F241-F244.
[3] V.V. Belousov, S.V. Fedorov, A.V. Vorobiev, The oxygen permeation of solid/melt composite $BiVO_4$ – 10 wt % V_2O_5 membrane, J. Electrochem. Soc. 158 (2011) B601-B604.
[4] I.V. Kul'bakin, V.V. Belousov, S.V. Fedorov, A.V. Vorobiev, Solid/melt ZnO – Bi_2O_3 composites as ion transport membranes for oxygen separation from air, Mater. Lett. 67 (2012) 139-141.
[5] I.V. Kul'bakin, S.V. Fedorov, A.V. Vorobiev, V.V. Belousov, Transport properties of ZrV_2O_7 – V_2O_5 composites with liquid-channel grain boundary structure, Russ. J. Electrochem. 49 (2013) 878-882.
[6] V.V. Belousov, Oxygen-permeable membrane materials based on solid or liquid Bi_2O_3, MRS Commun. 3 (2013) 225-233.
[7] V.V. Belousov, Liquid-channel grain-boundary structures with ionic-conduction, Russ. J. Electrochem. 31 (1995) 1240-1244.
[8] V.V. Belousov, Liquid-channel grain-boundary structures, J. Am. Ceram. Soc. 79 (1996) 1703-1706.
[9] V.V. Belousov, S. V. Fedorov, Accelerated mass transfer involving the liquid phase in solids, Russ. Chem. Rev. 81 (2012) 44-64.
[10] V.V. Belousov, Surface ionics: A brief review, J. Eur. Ceram. Soc. 27 (2007) 3459-3467.
[11] N. Nagbhushana, T. Nithyanantham, S. Bandopadhyay, J. Zhang, Subcritical crack growth behavior of a perovskite-type oxygen transport ceramic membrane, Int. J. Appl. Ceram. Technol. 8 (2011) 390-397.
[12] K. Partovi, F. Liang, O. Ravkina, J. Caro, High-flux oxygen-transporting membrane $Pr_{0.6}Sr_{0.4}Co_{0.5}Fe_{0.5}O_{3-\delta}$: CO_2 stability and microstructure, ACS Appl. Mater. Interfaces 6 (2014) 10274-10282.
[13] X. Zhu, W. Yang, Composite membrane based on ionic conductor and mixed conductor for oxygen permeation, AIChE J. 54 (2008) 665-672.
[14] V.V. Belousov, V.A. Schelkunov, S.V. Fedorov, I.V. Kul'bakin, A.V. Vorobiev, Oxygen-permeable In_2O_3-55 wt.% δ-Bi_2O_3 composite membrane, Electrochem. Commun. 20 (2012) 60-62.
[15] V.V. Belousov, V.A. Schelkunov, S.V. Fedorov, I.V. Kul'bakin, A.V. Vorobiev, Oxygen-permeable NiO/54 wt% δ-Bi_2O_3 composite membrane, Ionics. 18 (2012) 787-790.

[16] V.V. Belousov, Wetting of grain boundaries in ceramic materials, Colloid. J. 66 (2004) 121-127.
[17] V.V. Belousov, Grain boundary wetting in ceramic cuprates, J. Mater. Sci. 40 (2005) 2361-2365.
[18] V.V. Belousov, High-temperature solid/melt nanocomposites, JETP Lett. 88 (2008) 297-298.
[19] V. R. Yarlagadda, T. V. Nguyen, Conductivity measurements of molten Bi_2O_3, ECS Trans. 33 (2011) 119-125.
[20] T. Bak, J. Nowotny, M. Rekas, C.C. Sorrell, P.A. Banda, W. Wlodarski, Electrical conductivity of indium sesquioxide thin film, J. Mater. Sci. 13 (2002) 571-579.
[21] H.J.M. Bouwmeester, H. Kruidhof, A.J. Burggraaf, Importance of the surface exchange kinetics as rate limiting step in oxygen permeation through mixed-conducting oxides, Solid State Ionics 72 (1994) 185-194.
[22] P. Zeng, Z. Chen, W. Zhou, H. Gu, Z. Shao, S. Liu, Re-evaluation of $Ba_{0.5}Sr_{0.5}Co_{0.8}Fe_{0.2}O_{3-\delta}$ perovskite as oxygen semi-permeable membrane, J. Membr. Sci. 291 (2007) 148-156.
[23] K. Efimov, T. Klande, N. Juditzki, A. Feldhoff, Ca-containing CO_2-tolerant perovskite materials for oxygen separation, J. Membr. Sci. 389 (2012) 205-215.